.

Towards a Laser System for Narrow Line Cooling of Ytterbium Atoms

Jana Kalista Smith

A thesis submitted in partial fulfillment of
the requirements for the degree of

Master of Science

University of Washington

2009

Program Authorized to Offer Degree: UW Physics

University of Washington
Graduate School

This is to certify that I have examined this copy of a master's thesis by

Jana Kalista Smith

and have found that it is complete and satisfactory in all respects,
and that any and all revisions required by the final
examining committee have been made.

Committee Members:

_____

Subhadeep Gupta

_____

Stephen R. Sharpe

Date: _____

University of Washington

Abstract

Towards a Laser System for Narrow Line Cooling of Ytterbium Atoms

Jana Kalista Smith

Chair of the Supervisory Committee:
Professor Subdaheep Gupta
Department of Physics

this is where an abstract goes

TABLE OF CONTENTS

Page

LIST OF FIGURES

LIST OF TABLES

Chapter 1

INTRODUCTION

Many advances have been made in the area of ultracold atoms and quantum degenerate gases over the past two decades, some of which led to Nobel prizes in 1997 for laser cooling and in 2001 for Bose-Einstein Condensation. Such success with atoms has led to an interest in investigating molecules.

Ultracold and quantum degenerate polar molecules have strong dipole-dipole interactions. It is predicted these molecules will give rise to a variety of new condensed phases such as BCS-like p-wave superfluids for fermions [1], and supersolid and checkerboard states for bosons [2]. They have also been proposed as qubits of a scalable quantum computer [3]. The molecular degrees of freedom also allow for improvements for precision measurements including tests of fundamental symmetries [4] and tests of temporal variations of fundamental constants [5, 6].

One route to ultracold molecules is to link cooled atoms together via photoassociation (PA) or Feshbach resonances (FB). Photoassociation to a molecular ground state requires coupling two free atoms to an excited state molecule with a single photon. The molecule then decays to a rotational-vibrational state by either spontaneous (1 photon PA) or stimulated (2 photon PA) emission. When two free atoms collide with an energy coinciding with the energy of a bound molecular state a Feshbach resonance occurs. The energy of the atomic collision and molecular state are tuned by an external magnetic field. These techniques have been adopted with success in creating different species of homonuclear [7, 8, 9, 10] and heteronuclear [11, 12, 13] molecules.

The atoms selected for this experiment are lithium (Li) and ytterbium (Yb). There are many reasons why these atoms were chosen. Both types of atoms have been brought to quantum degeneracy individually using standard techniques of laser and evaporative cooling [14, 15, 16, 17, 18]. Also both have fermionic and bosonic isotopes so a variety of

combinations can be used to make bosonic or fermionic molecules. A large electric dipole moment is expected due to their large difference in mass and electronic structure. The paramagnetic lithium and diamagnetic ytterbium gives a finite magnetic moment in the molecular ground state allowing the molecule to be trapped magnetically.

A dual-species Magneto-Optical Trap (MOT) is the workhorse of the experiment. Setting up the trap requires laser light at frequencies specific to the atoms, there will have to be several different laser systems. Lithium has a strong atomic transition at 671 nm. Ytterbium has a broad line at 399 nm and a narrow 556 nm intercombination line. The laser system for the green 556 nm transition of ytterbium is the focus of this thesis.

Chapter 2

EXPERIMENT

2.1 Experimental Set-up

The lithium (Li) and ytterbium (Yb) atoms will be laser cooled in the same spatial location. This will be done in a dual-species Magneto-Optical Trap (MOT). Atomic beams will be loaded into the ultrahigh vacuum chamber of the MOT by two Zeeman slowers, one for each species. There they will be trapped and undergo evaporative cooling. Temperatures of 150 μK in Li [15] and 40 μK in Yb [16, 19] can be reached by using laser cooling techniques. To cool the atoms further they will be confined in a far-off resonant trap (FORT) while evaporative cooling is performed. The molecules will be made by photoassociation process with a laser tuned near the Li resonant frequency.

2.2 Ytterbium

Ytterbium a soft, malleable element with a silvery appearance. It is fairly stable, but should be stored in a closed container to protect it from air and water. It is a rare earth element with atomic number is 70 and its ground state electron configuration is [Xe]$4f^{14}6s^2$. It has seven stable isotopes, five are bosonic (even) with $I = 0$ and two are fermionic (odd) with $I = 1/2, 5/2$. The isotopes, their nuclear spin, and natural abundance can be seen in Table 2.1. Ytterbium's narrow intercombination line make it a good candidate for studies including optical clocks, new quantum phases, and quantum information.

The energy levels of ytterbium relevant to the experiment are displayed in Fig. 2.1. There is a strong $6s^2\ {}^1S_0 \rightarrow 6s6p\ {}^1P_1$ transition at 399 nm which has a broad linewidth of $2\pi \times 29$ MHz. This can be used to Zeeman slow the atoms, but it isn't a good transition for the MOT. Atoms in the ${}^1P_1$ state have a probability of decaying into metastable triplet states. This branching gives a limitation on the lifetime and number of trapped atoms in the MOT. This transition also has a high Doppler limit. There is a closed transition which

Table 2.1: Natural abundance and nuclear spin of Yb.

Isotope	Natural Abundance	Nuclear Spin
^{168}Yb	0.0013	0
^{170}Yb	0.0305	0
^{171}Yb	0.143	1/2
^{172}Yb	0.219	0
^{173}Yb	0.161	5/2
^{174}Yb	0.318	0
^{176}Yb	0.127	0

can be used for a MOT. It is the weaker intercombination transition, $6s^2\ {}^1S_0 \rightarrow 6s6p\ {}^3P_1$, at 556 nm. This has a narrow linewidth of $2\pi \times 182$ kHz.

2.3 Green Laser Systems

To cool and trap ytterbium using the ${}^1S_0 \rightarrow {}^3P_1$ transition a laser is needed at 556 nm. At this particular wavelength there used to be only one choice for a laser system. This was a frequency-stabilized dye laser (with rhodamine 560 chloride (formerly named rhodamine 110) dye). Dye lasers are known to be inefficient, bulky, and needing frequent maintenance. The lasing medium is a moving dye so much care must be given to ensure smooth dye flow. Another problem with the dye laser is it has a linewidth of about 1 MHz. The ${}^1S_0 \rightarrow {}^3P_1$ transition's narrow linewidth requires the laser to be stabilized to < 200 kHz.

The second option for a laser system is to use second harmonic generation (SHG) to frequency double 1112 nm light to 556 nm. Although diodes don't exist at 556 nm they are commonly found in the infrared region and are relatively inexpensive. These lasers are low-maintenance and have narrow linewidths and high power output. Therefore, if enough power can be produced at the second harmonic wavelength this is the superior choice.

One option for frequency doubling is to send the fundamental beam through a periodically poled nonlinear crystal. These ferroelectric crystals have a periodic reversal of the

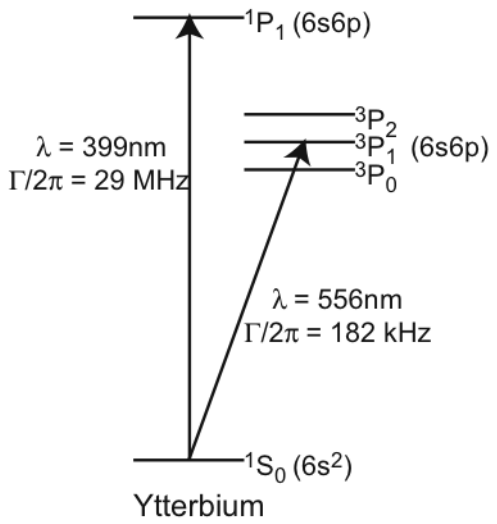

Figure 2.1: Energy level diagram for ytterbium. tHe broad 399 nm transition will be used for a Zeeman slower beam and the narrow 556 nm transition will be used for the MOT beams.

orientation of their domains with a period which is wavelength and temperature dependent. This gives a 180° phase shift in the generated second harmonic. As the light travels through the crystal the structure is inverted when the second harmonic is a maximum. This causes the light generated past this point to add constructively with the existing harmonic. This is designed to achieve quasi-phase matching in the crystal. Periodically poled crystals are somewhat limited in variety and expensive given their conversion efficiency.

Another option is to place a nonlinear crystal in an optical cavity. The crystal may be placed in the laser's cavity or in an external cavity. The light circulating the cavity makes multiple passes through the crystal increasing its second harmonic conversion. There is a commercial laser by Toptica available which uses this method, however they give an outpower of < 15 mW. Recently conversion efficiencies of up 58% have been reported at this wavelength [20] using this method.

With all this considered SHG of light from a 1112 nm diode pumped 1 Watt fiber laser with a homemade external resonant cavity has been chosen for the green laser system.

Potassium niobate ($KNbO_3$) is the type of crystal chosen. Lithium triborate (LBO) is a common choice for SHG. At out wavelength it has a second harmonic coefficient of 0.654 pm/V and a walk-off angle of 0.3°. $KNbO_3$ has a second harmonic coefficient of 8.69 pm/V and a walk-off angle of 3°. Although $KNbO_3$ has a higher walk-off than LBO it was chosen for it's higher second harmonic coefficient. The next two chapters of this thesis outline the theory and experimental design of the system.

Chapter 3

THEORY AND DESIGN OF A HIGH POWER DOUBLING CAVITY

This chapter gives a brief coverage of theoretical considerations needed to build an efficient second harmonic generation (SHG) resonant cavity. It starts out with background on ideal Gaussian beams which are a good approximation for the laser beam used in this experiment. Next, the theory of SHG is covered. Finally, theory on optical resonators is discussed.

3.1 Gaussian Beams

A Gaussian beam is one with an intensity distribution that can be described by Gaussian functions. Lasers emit beams with a Gaussian profile called the fundamental transverse or TEM_{00} mode of the laser's optical resonator. The theory of Gaussian beams is a rich and interesting topic. Some basics are give here, detailed descriptions are given in textbooks such as Seigman's *Lasers* [21].

3.1.1 Overview of Gaussian Beams

Any optical wave must be a real function of position and time, $u(\mathbf{r}, t)$, which satisfies the wave equation

$$\left(\nabla^2 - \frac{1}{c^2}\frac{d^2}{dt^2}\right) u(\mathbf{r}, t). \tag{3.1}$$

In order to solve this equation we take $u(\mathbf{r}, t)$ to be the real part of the complex function

$$U(\mathbf{r}, t) = U(\mathbf{r})e^{2i\pi\nu t}, \tag{3.2}$$

where ν is the frequency of the wave. Inserting (3.2) into (3.1) gives the Helmholtz equation,

$$\left(\nabla^2 + k^2\right) U(\mathbf{r}, t) = 0, \tag{3.3}$$

where $k = 2\pi\nu/c = \omega/c$ is called the wave number. There are many solutions to this equation, the most useful is the Gaussian beam.

A wave is paraxial if its wavefront normals are paraxial rays, those which make small angles relative to an optical axis. It can be represented by a plane wave

$$U(\mathbf{r}) = A(\mathbf{r})e^{ikz}, \tag{3.4}$$

where $A(\mathbf{r})$ is the slowly varying amplitude of the wave. In this slowly varying envelope approximation changes in A are much smaller than A and (3.3) becomes

$$\nabla_T^2 A + 2k\frac{dA}{dz} = 0. \tag{3.5}$$

Here $\nabla_T^2 = \frac{\partial^2}{\partial x^2} + \frac{\partial^2}{\partial y^2}$ is the transverse Laplacian. The Gaussian beam solution to this equation gives

$$A(\mathbf{r}) = \frac{A_0}{q(z)} exp\left[ik\frac{x^2+y^2}{2q(z)}\right], \tag{3.6}$$

where A_0 is a constant. $q(z)$ is a complex parameter given by

$$\frac{1}{q(z)} = \frac{1}{R(z)} + i\frac{\lambda}{\pi w(z)}. \tag{3.7}$$

The beam radius or spot size $w(z)$ is given by

$$w(z) = w_0\left[1+\left(\frac{z}{z_0}\right)^2\right]^{1/2}. \tag{3.8}$$

The beam radius $w(z)$ is a minimum at w_0, this is called the beam waist and is given by

$$w_0 = \left(\frac{\lambda z_0}{\pi}\right)^{1/2}. \tag{3.9}$$

z_0 is known as the Rayleigh range which is the distance from the beam waist over which the beam radius is increased by $\sqrt{2}$. The confocal parameter or depth of focus of the beam, b, is given by

$$b = 2z_0 = \frac{2\pi w_0^2}{\lambda}. \tag{3.10}$$

The radius of curvature of the beam is

$$R(z) = z\left[1+\left(\frac{z_0}{z}\right)^2\right]. \tag{3.11}$$

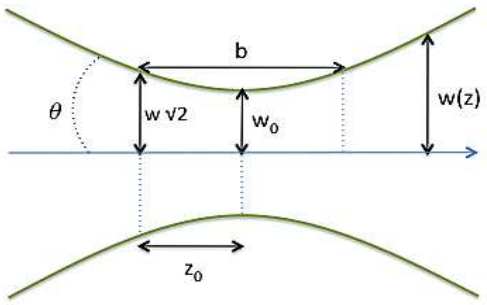

Figure 3.1: Parameters of a Gaussian beam.

The beam radius spreads out as the wave propagates away from the waist. $w(z)$ approaches a straight line as $z >> z_0$. The angle between this line and the optical axis is called the divergence of the beam and is given by

$$\theta \simeq \frac{\lambda}{\pi w_0}. \tag{3.12}$$

These quantities are used to determine the properties of the Gaussian beam and demonstrated in Fig. 3.1.

3.1.2 Matrix Methods for Gaussian Beams

As a beam propagates it may encounter a series of lenses, mirrors, free space, etc. These may cause the beam parameters to change. Resonant cavities have a number of optical components so it is desirable to have a simple way to keep track of the beam shape. Information on how an optical component causes a beam to change can be stored in a matrix specific to that component. To describe the total path traversed one multiplies the matrices of each component together. This gives a system matrix for the entire optical system, written symbolic form as

$$M = \begin{bmatrix} A & B \\ C & D \end{bmatrix}. \tag{3.13}$$

The determinant of the system matrix has the useful property of

$$AD - BC = \frac{n_0}{n_f}, \tag{3.14}$$

where n_0 and n_f are the refractive indicies of the initial and final medium, respectively. Usually one is dealing with rays starting and ending in the same medium so the determinant is equal to unity.

The simplest example of one of these matrices gives the propagation of a beam through free space, called a translation matrix. Consider a single normal to a wavefront, a paraxial ray. This ray may be characterized by the distance y from and the angle α to the optical axis. As the beam moves through a distance L the angle remains the same, but the distance from the axis changes to some final value y_f. These can be quantified by the following equations put in a suggestive form

$$\begin{aligned} y_f &= (1)y_0 + (L)\alpha_0 \\ \alpha_f &= (0)y_0 + (1)\alpha_0, \end{aligned} \tag{3.15}$$

where the small angle approximation $\tan\alpha_0 \simeq \alpha_0$ has been used and y_0, α_0 describe the initial position and angle. The equations can be written in matrix form

$$\begin{bmatrix} y_f \\ \alpha_f \end{bmatrix} = \begin{bmatrix} 1 & L \\ 0 & 1 \end{bmatrix} \begin{bmatrix} y_0 \\ \alpha_0 \end{bmatrix}. \tag{3.16}$$

The 2×2 matrix is the translation matrix. Matrices for other optical components a beam can encounter can be derived similarly.

Matrix methods can be used to describe the propagation of Gaussian beams as well as optical rays. A system matrix for some optical set-up relates the outgoing beam to the incoming beam by

$$\begin{bmatrix} y_f \\ \alpha_f \end{bmatrix} = \begin{bmatrix} A & B \\ C & D \end{bmatrix} \begin{bmatrix} y_0 \\ \alpha_0 \end{bmatrix}. \tag{3.17}$$

For a Gaussian beam the ABCD propagation law is given by,

$$q_f = \frac{Aq_0 + B}{Cq_0 + D}, \tag{3.18}$$

where q is given by (3.7). This relationship allows one to describe the outcoming shape of a Gaussian beam after it passes through an arbitrary optical system. If the incoming beam

parameter is known along with the system matrix, the outgoing beam parameter can be found with (3.18).

3.2 Second Harmonic Generation

Second harmonic generation (SHG) or frequency doubling is the process in which light is sent through a nonlinear medium to produce light at twice the frequency of the fundamental. This section starts out with a brief overview of nonlinear optics. It then introduces phase matching which is crucial for getting maximum SHG power out of a crystal.

3.2.1 Nonlinear Optics

As a beam of light propagates through a medium, the electric field applies a force on the electrons of the atoms which make up the medium. This force causes a separation of the positively charged nucleus and the negatively charged electrons. As a result of this charge separation an electric dipole moment is formed and given by

$$\mathbf{p} = e\mathbf{d}, \tag{3.19}$$

where e is the fundamental electron charge and $\mathbf{d}$ is the separation between the charges. The dipole moment per unit volume is called the polarization of the medium and is given by

$$\mathbf{P} = \epsilon_o \chi \mathbf{E}. \tag{3.20}$$

Here ϵ_o is the permittivity of free space, $\mathbf{E}$ is the applied electric field, and χ is a constant dependent on the medium called the electric susceptibility. Equation 3.20 shows that if $\mathbf{E}$ oscillates, so does $\mathbf{P}$. The oscillation of $\mathbf{P}$ indicates the medium is now composed of a bunch of oscillating dipoles which emit radiation. The relationship between $\mathbf{E}$ and $\mathbf{P}$ is linear for small applied fields, but becomes nonlinear as $\mathbf{E}$ acquires values comparable to interatomic electron fields. An intense light beam can generate nonlinear optical effects just as a mass on a spring can be mechanically overdriven into a nonlinear response. This has been empirically confirmed with great aid from the invention of the laser.

To see how a nonlinear relationship arises to give harmonics consider the one dimension case. Start by expanding equation (3.20) in a Taylor series about $E = 0$ to get

$$P = \chi_1 E + \chi_2 E^2 + \chi_3 E^3 + ... \tag{3.21}$$

where

$$\chi_1 > \chi_2 > \chi_3. \tag{3.22}$$

Take the oscillating electric field to be of the form

$$E = E_o \sin \omega t \tag{3.23}$$

and plug into (3.21). With some trig. manipulation it becomes

$$P = \chi_1 E_o \sin \omega t + \frac{\chi_2 E_o^2}{2}(1 - \cos 2\omega t) + \frac{\chi_3 E_o^3}{4}(3 \sin \omega t - \sin 3\omega t) + ... \tag{3.24}$$

The arguments of the trig. functions indicate that as the field passes through the medium it creates a polarization wave at different frequencies. The linear term represents the refracted wave. The second term represents one with a dc component and which oscillates at twice the fundamental frequency. The higher order terms give rise to the higher harmonics. The above is a simplified case for one dimension. In reality **E** and **P** are vectors and χ is a tensor, not a scalar. This makes the math more complicated, but the same general idea applies. χ_2 is called the effective nonlinear coefficient or the second harmonic coefficient. It is often notated as d_{eff} and will be referred to as such for the remainder of this thesis.

3.2.2 Phase Matching

The generated power at twice the frequency of the fundamental beam of a plane wave in a nonlinear medium can be derived from Maxwell's equations and is given by [22]

$$P_{2\omega} = 2 \left(\frac{\mu_0}{\epsilon_0} \right)^{3/2} \frac{\omega^2 l^2 d_{eff}^2}{n^3 A} \left(\frac{\sin(\Delta k l/2)}{\Delta k l/2} \right)^2 P_\omega. \tag{3.25}$$

Here ω is the frequency of the fundamental beam, P_ω is the power of the fundametal beam, d_{eff} is the second harmonic coefficient, l is the length of the crystal, A is the area of the incident beam, n is the fundamental index of refraction of the medium, and $\Delta k = k_2 - 2k_1$ is

the phase mismatch between the wave numbers of the second harmonic and the fundamental beam. The second harmonic power is maximized when $[\sin(\Delta kl/2)/(\Delta kl/2)]^2$ is maximum which happens when Δk is a minimum. The efficiency of nonlinear conversion grows with distance along the medium, but the wave vectors need to be matched. Second harmonic conversion is maximized by minimizing the difference between the indicies of refraction of the fundamental and the second harmonic in the medium. This is called phase matching and can be done by using a birefringent crystal.

Birefringent crystals have the property that the index of refraction depends on the polarization direction of the wave travelling through them. When a light wave enters a birefringent crystal it is divided into two waves called the ordinary and extraordinary wave. Ordinary waves, waves with polarization perpendicular to the optical axis, have fixed index of refraction independent of direction. Extraordinary waves, waves with polarization in the plane of the optical axis, have an index of refraction which depends on the direction of propagation to the optical axis. These indicies can be tuned by adjusting either the temperature of the crystal (noncritical phase matching) or the angle of wave propagation in the crystal (critical phase matching).

Angle phase matching can be achieved by changing the angle between the optical axis of the crystal and the directions of propagation of the beams. For example, the input fundamental beam may propagate as the ordinary beam giving it an index of refraction $n_{o,\omega}$ while the second harmonic propagates as the extraordinary beam with index of refraction $n_{e,2\omega}$.

The extraordinary waves have an index of refraction which depends on the angle, *theta*, of propagation to the optical axis given by

$$n_{e,\omega}(\theta) = \left[\frac{\sin^2\theta}{n_{e,\omega}^2} + \frac{\cos^2\theta}{n_{o,\omega}^2}\right]^{-1/2}. \tag{3.26}$$

When phase matching is achieved

$$n_{e,2\omega}(\theta) = n_{o,\omega}. \tag{3.27}$$

Table 3.1: Indicies of refraction for 1112 and 556 nm in the three cardinal directions of the crystal.

n	1112 nm	556 nm
n_z	2.2542	2.3660
n_y	2.2167	2.3102
n_x	2.1171	2.1931

Inserting (3.27) into (3.26) and some manipulation gives the phase matching angle as

$$\theta_m = \sin^{-1}\sqrt{\frac{n_{o,\omega}^{-2} - n_{o,2\omega}^{-2}}{n_{e,2\omega}^{-2} - n_{o,2\omega}^{-2}}}. \tag{3.28}$$

To find the phase matching angle it is necessary to first find the indicies of refraction for our wavelengths in our $KNbO_3$ crystal. Zysset, Biaggio, and Günter [23, 24] have done extensive studies on $KNbO_3$ and they supply the necessary numbers for carrying out this operation. The indicies of refraction in the x, y, and z directions for 1112 and 556 nm are found by Sellmeier's equations,

$$n = \left(1 + S1\frac{\lambda^2\lambda1^2}{\lambda^2 - \lambda1^2} + S2\frac{\lambda^2\lambda2^2}{\lambda^2 - \lambda2^2} - \mu\lambda^2\right)^{1/2} \tag{3.29}$$

where λ is the wavelength at which the index of refraction is being calculated,$S1$ and $S2$ are the oscillator strengths, $\lambda1$ and $\lambda2$ represent positions of the UV oscillator terms, and μ is the coefficient of an IR correction term. The found indicies are listed in Table 3.1.

For a negative biaxial crystal such as $KNbO_3$ it is the case that $n_{e,2\omega} < n_{o,\omega}$ so we have

$$\begin{aligned} n_z &= n_{o,\omega} = 2.254 \\ n_y &= n_{o,2\omega} = 2.310 \\ n_x &= n_{e,2\omega} = 2.193. \end{aligned} \tag{3.30}$$

Plugging these values into (3.28) gives $\theta_m = 42.6°$. A graph of refractive index vs. wavelength (3.29) has been plotted in Fig. 3.2. The straight line has been drawn at $n = 2.254$ to show the two indicies are equal at 1112 and 556 nm.

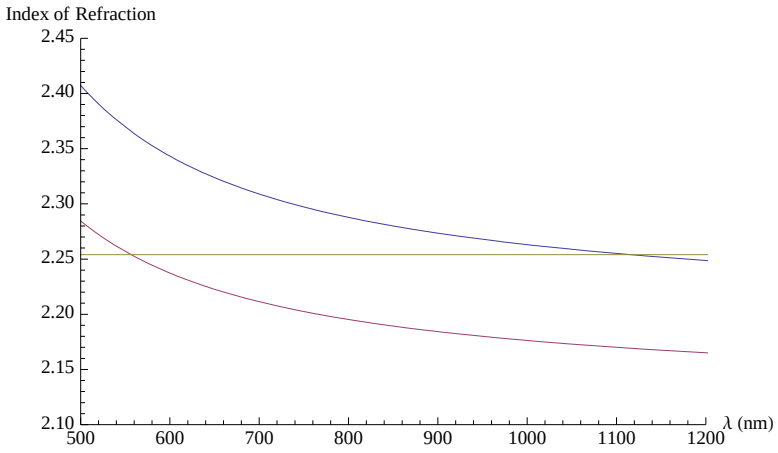

Figure 3.2: Graph of index of refraction vs. wavelength for the ordinary fundamental (top blue curve) and the extraordinary second harmonic (bottom red curve). The horizontal line is at $n = 2.254$, notice it intersects the two curves at 1112 and 556 nm.

One disadvantage of angle phase matching is there is a so-called walk-off angle. This occurs because the Poynting vectors are in general not parallel to the wave vectors as the wave moves along the crystal. This causes the energy flow of the wave to diverge from the direction of propagation. The walk-off angle is given as

$$\rho = \tan^{-1}\left(\frac{1}{2}n_{o,\omega}^2 \sin 2\theta[n_{e,2\omega}^{-2} - n_{o,2\omega}^{-2}]\right). \tag{3.31}$$

It is advantageous to choose a crystal with a small walk-off angle at the required wavelength. This also puts a limit on how long the crystal can be. $KNbO_3$ has $\rho = 2.98^\circ$ for our wavelengths.

3.2.3 SHG with Gaussian Beams

It is desired to optimize the SHG light generated. The theory of second harmonic generation with focused Gaussian beams has been developed in detail by Boyd and Kleinman [25]. They find the optimal focal properties of the fundamental beam given the crystal length, refractive index, and the walk-off angle. The SHG power is is found by integrating over the full crystal to add up all the sources of the second harmonic beam. If the Gaussian beam has its waist

in the center of the crystal then it can be approximated as a plane wave. The outcoming second harmonic power is found to be

$$P_{2\omega} = KP_{\omega}^2 l k_{\omega} e^{\alpha' l} h(\sigma, \beta, \kappa, \xi, \mu), \tag{3.32}$$

where

$$K = \frac{128\pi^2\omega_1^2}{c^2 n_1^2 n_2} d_{eff}^2 \tag{3.33}$$

and α' is the absorption of the crystal. The function $h(\sigma, \beta, \kappa, \xi, \mu)$ contains all of the optimizable parameters defined as

$$\begin{array}{cc} \text{phase mismatch} & \sigma = \frac{1}{2} b \Delta k \\ \text{focal position} & \mu = (l - 2f)/l \\ \text{strength of focussing} & \xi = l/b \\ \text{double refraction} & \beta = B\xi^{-1/2} \\ \text{absorption} & \kappa. \end{array} \tag{3.34}$$

l is the optical length of the crystal, $b = 2\pi\omega_o^2/\lambda$ is the confocal parameter, and $B = \frac{1}{2}\rho\sqrt{lk}$ is the walk-off parameter where ρ is the walk-off or double refraction angle. Boyd and Kleinman assume no absorption so the focal position is optimized at the center of the crystal and $\kappa = \mu = 0$.

In order to determine the length choice for the crystal B was calculated for several different lengths. All of these were greater than 9 for our set-up. Boyd and Kleinman find for values of B greater than 6 the strength of focussing has a maximum value given by

$$\xi = \frac{l}{b} = 1.39. \tag{3.35}$$

This means $h(B, \xi)$ is also a maximum. Although the length of the crystal dictates parameters of the cavity, it doesn't affect maximum power of SHG in our system greatly. We can calculate the waist wanted in the crystal by (3.35). For a crystal of length 5 mm this comes out to be 38 μm.

3.3 Optical Resonators

An optical resonator or cavity consists of two or more mirrors arranged to allow light to propagate along a closed path. The simplest version, known as a Fabry-Perot resonator

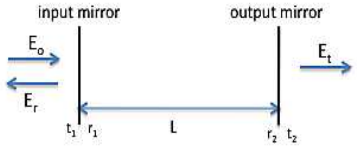

Figure 3.3: Diagram of a Fabry-Perot etalon.

or interferometer, has two mirrors facing each other and creates a standing wave between them. Most cavities used today for SHG are ring cavities which have three or more mirrors.

3.3.1 Two Mirror Cavity

To demonstrate how a resonator works it is useful to first consider the simplest version of a resonant cavity, the Fabry-Perot etalon. It consists of two planar mirrors separated by a distance L. A mirror is characterized by its field amplitude reflection coefficient r and its transmission coefficient t. Usually the intensity reflectivity $R = |r^2|$ and transmission $T = |t^2|$ are the quantities of interest. Mirrors are not perfect, they absorb and scatter a small fraction of incident light. These losses can be lumped together and described by a single variable $\mathcal{L}$. Conservation of energy necessitates that $R + T + \mathcal{L} = 1$, which becomes $R + T = 1$ for ideal mirrors.

In order to characterize the field inside and transmitted by a cavity, consider a laser beam incident on a two mirror cavity as in Fig. 3.3. The laser has a field intensity E_0 and frequency ν with corresponding wave number k. Each mirror has amplitude reflectivity r and transmission t. The incident laser beam passes through the back of the first mirror so just to the right of this input coupler the field amplitude is

$$E_{c_0} = t_1 E_0. \tag{3.36}$$

The light then travels the length L of the cavity and is partially reflected off of the second mirror, called the output coupler. It then returns to the first mirror and is partially reflected

again to give the original wave a complete round trip amplitude of

$$E_{c_1} = t_1 E_0 r_1 r_2 e^{2ikL}, \tag{3.37}$$

where $2kL$ is the round trip phase shift. After another round trip the field is

$$E_{c_2} = t_1 E_0 (r_1 r_2)^2 e^{4ikL}. \tag{3.38}$$

The wave continues bouncing between the mirrors in this fashion to give an amplitude after n round trips of

$$E_{c_n} = t_1 E_0 (r_1 r_2)^n e^{2inkL}. \tag{3.39}$$

Thus the total field can be written as the sum of the fields after each round trip. This is a geometric series with the sum

$$E_c = t_1 E_0 \sum_{n=0}^{\infty} (r_1 r_2)^n e^{2inkL} = \frac{t_1 E_0}{1 - r_1 r_2 e^{2ikL}}. \tag{3.40}$$

This gives the intensity in the cavity as

$$I_c = |E_c|^2 = \frac{T_1 I_0}{1 + R_1 R_2 - 2\sqrt{R_1 R_2}\cos(2kL)}. \tag{3.41}$$

It is also of interest to find the intensity of the transmitted and reflected beams. The electric field and intensity transmitted through the output coupler is given by

$$E_t = \frac{t_1 t_2 e^{ikL}}{1 - r_1 r_2 e^{2ikL}} E_0 \tag{3.42}$$

$$I_t = \frac{T_1 T_2}{1 + R_1 R_2 - 2\sqrt{R_1 R_2}\cos(2kL)} I_0 \tag{3.43}$$

The reflected beam from the input coupler has two contributions. The first term is the beam directly reflected and the second comes from the light transmitted back out of the cavity through the input coupler. The reflected electric field and intensity are given by

$$E_r = \left[-r_1 + \frac{r_2 T_1 e^{2ikL}}{1 - r_1 r_2 e^{2ikL}} \right] E_0 \tag{3.44}$$

$$I_r = \frac{|-1 + [1 + \frac{T_1}{R_1}]\sqrt{R_1 R_2} e^{2ikL}|^2}{1 + R_1 R_2 - 2\sqrt{R_1 R_2}\cos(2kL)} R_1 I_0. \tag{3.45}$$

The two components of (3.44) indicate it must be the case that $r_1 = r_2(R_1 + T_1)$ in order for the total reflected field to be zero. If this is the case the cavity is said to be impedance

matched. If $r_1 < r_2(R_1+T_1)$ the cavity is overcoupled and the field coming out of the cavity overpowers the reflection. If $r_1 > r_2(R_1+T_1)$, the cavity is undercoupled and the reflection from the input coupler dominates the light leaking out of the cavity.

If the reflectance and transmittance of the mirrors is taken to be the same, then for lossless mirrors (3.43) and (3.45) become

$$\frac{I_t}{I_0} = \frac{(1-R)^2}{1+R^2-2R\cos(2kL)} = \frac{(1-R)^2}{(1-R)^2+4R\sin^2(kL)} \tag{3.46}$$

$$\frac{I_r}{I_0} = \frac{2R(1-\cos(2kL))}{1+R^2-2R\cos(2kL)} = \frac{4R\sin^2(kL)}{(1-R)^2+4R\sin^2(kL)}, \tag{3.47}$$

where the trig. identity $\cos\delta = 1-2\sin^2\frac{\delta}{2}$ has been used. These are known as Airy's functions. Fig. 3.4 shows a plot of these functions versus phase for three different R values. Note that there are instances of almost no reflection and total transmission. These occur at the resonant frequencies of the cavity under the condition $2kL = 2m\pi$, where m is an integer. These modes can be achieved by varying the frequency of the laser and/or the length of the cavity.

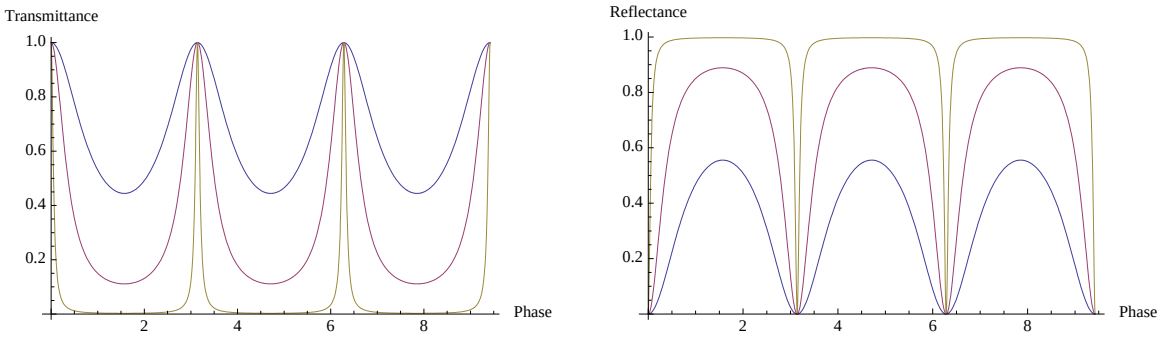

Figure 3.4: Graph of transmitted intensity vs. phase (left) and reflected intensity vs. phase (right) for a Fabry-Perot cavity for three different values of R. For the transmittance graph the top blue line is for $R = 0.2$, the middle red curve is for $R = 0.5$, and the bottom yellow curve is for $R = 0.9$. The order from top to bottom is reversed for the reflectance graph.

This experiment uses a ring cavity instead of a two mirror cavity, however, it has similar resonant modes. The main difference in quantities introduced above is there are more mirrors the light is reflecting off of so there are more reflection coefficients introduced. Ring

cavities are desireable because they allow light to travel in only one direction around the cavity. This is good because it ensures no reflection directly back into the laser. For SHG is is benefical because the SHG occurs in one direction and only a single pass through the crystal contributes to loss.

3.3.2 Resonator Characteristics

Some useful quantities used to characterize a cavity are introduced below. The free spectral range (FSR) of a cavity is the frequency spacing between the m and $m+1$ cavity modes. It is given by $FSR = c/2L$ for a two mirror cavity. A ring cavity has $FSR = c/L$, where L is the full length of the cavity.

The enhancement of a perfectly aligned and mode-matched cavity is

$$A = \frac{1-R}{(1-\sqrt{RV})^2}, \tag{3.48}$$

where R is the reflectivity of the IC and V is the total fraction of power remaining in the cavity after one round trip. The enhancement is maximized when $R = V$,

$$A = \frac{1}{1=V}. \tag{3.49}$$

The finesse of the cavity is given by

$$F = \frac{\pi(RV)^{1/4}}{1-\sqrt{RV}}. \tag{3.50}$$

If this condition is met the cavity is said to be impedence matched. The finesse is a numerical value which characterizes the width or sharpness of the maxima. It is given by the FSR/FWHM of the cavity's peaks. A high value of the finesse is an indication of a good cavity.

In order to excite the desired mode of an optical cavity it is necessary to focus the input beam using a lens to properly couple it to the desired transverse mode of the cavity. This is referred to as mode matching. If the input beam is not properly mode matched to the TEM_{00} mode then it will excite some mixture of low or high order transverse modes in the cavity. These must be minimized to get a good signal for the fundamental mode. The matrix methods and the ABCD law outlined in section 3.1.2 can be used to obtain the size

of the waists in the cavity. Once these are known a lens or series of lenses can be placed outside the cavity to achieve proper mode matching.

Chapter 4

CONSTRUCTION OF AN OPTICAL RESONATOR

The following gives a detailed description of components of the cavity to date. It includes our design of a bow-tie cavity and methods for obtaining an error signal to lock the cavity.

4.1 Fiber Laser System

The laser used for this system is an ytterbium-doped fiber laser. This turn-key system laser was manufactured by Koheras, it is the BoostiK system model number BoY10PztS. The laser operates in the wavelength range of 1111.45-1111.70 nm and puts out a maximum power of 1 W. The linewidth is specified by the manufacturer to be < 40 kHz, which is adequate for our narrow atomic transition. Although the performance of this fiber laser has been good, there have been drifts in the power and polarization. These come and go and change in their nature so no steps for correction have been taken.

The front panel of the laser allows for temperature and current control which adjust the frequency and power of the laser, respectively. The back panel has a remote interlock LEMO socket and the laser can be operated only when its two terminals are short circuited. There is also a LEMO socket PZT control connector on the back panel. This allows the frequency of the laser to be adjusted electronically. The PZT tuning coefficient is 20.6 MHz/V and the tuning range is 17 pm. A BNC connector has been soldered to the LEMO connector.

The laser output fiber is a 980 PM type standard single mode fiber with a FC/APC connector. This fiber has been damaged. Correspondence with a Koheras representative led us to believe there was a crack in the fiber core, usually due to dust being burned from the laser light. We decided to replace the connector ourselves to see if the beam output could be improved. New FC/APC single mode connectors with diameter 125μm were bought from Thorlabs (part number 30126F1) along with a connectorization kit. After the fourth attempt of reconnectorization we were able to retrieve 43% of laser light sent into a single

mode fiber back out. This shows the mode of the laser is well matched with the fundamental Gaussian mode. Although the beam output doesn't look perfect, Fig. 4.1, and the fiber tip appears to be scratched, it should be good enough to be matched into the cavity.

4.2 Potassium Niobate Crystal

The nonlinear crystal chosen for this experiment is Potassium Niobate ($KNbO_3$). It was chosen because it has a high second harmonic conversion coefficient ($d_{eff} = 8.69$ pm/V) at this wavelength and high damage threshold. It is nonhygroscopic like other commonly used nonlinear crystals. As described in section 3.2.1 the phase matching angle is 42.6°, the walk-off is 2.98°, and the index of refraction is 2.254.

Two of these crystals were bought from United Crystals Company. One is used in the cavity, the other is stored in the optics cabinet. The crystals are 5 mm in length and 3 mm in the other two dimensions. They have been antireflection coated for 1112 and 556 nm and placed in a mountable holder by United Crystals. In order for the polarization to be correct for phase matching the line across the holder should be perpendicular to the direction of the polarization of the incoming light. The holder is mounted in a standard mirror mount which is attached via a homemade plate to a Thorlabs miniature XYZ translation stage.

4.3 SHG Enhancement Cavity

4.3.1 Passive Isolation

The cavity's home is upon a $12'' \times 18''$ Thorlabs anodized aluminum breadboard which is $1/2''$ thick. In order to reduce vibrations to the cavity several measures were taken. The aluminum breadboard has a $1/4''$ thick brass plate underneath it and is secured to five $3''$ brass cylinders which are screwed into the optics table. In between the brass plate and cylinders is a layer of norbathene. The cavity is enclosed in a $20'' \times 16'' \times 12''$ plexiglass box with a removable lid. Several holes have been cut in this enclosure for beams and cords to enter and exit.

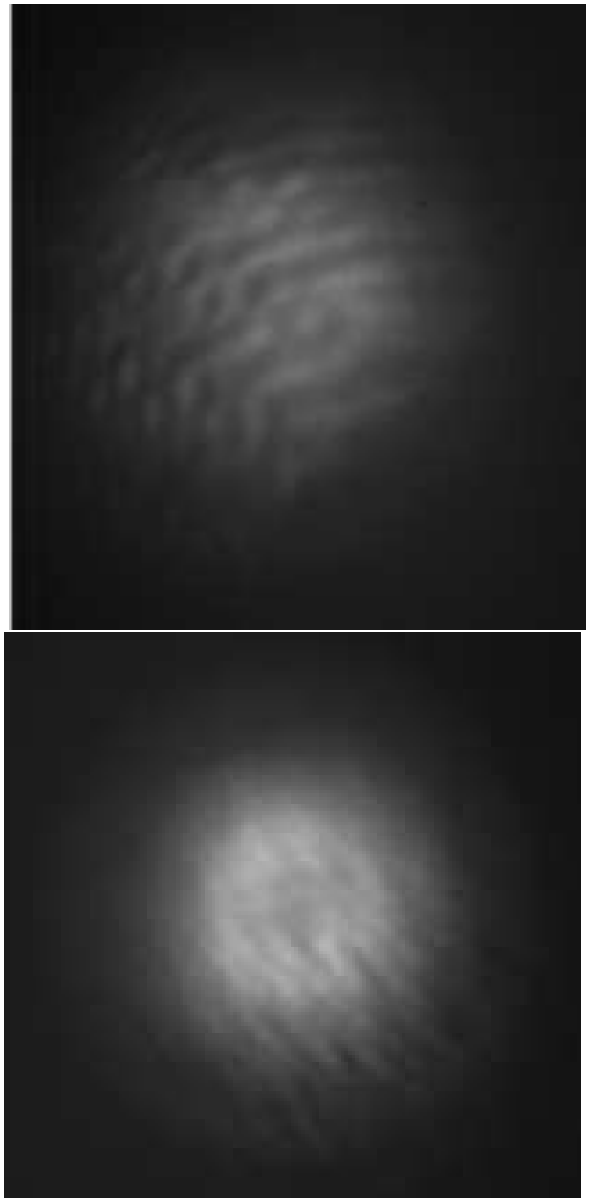

Figure 4.1: Pictures of laser output beams. The top photograph is of the fiber laser output beam. The bottom photograph is of an undamaged laser. It is included for reference of photograph quality.

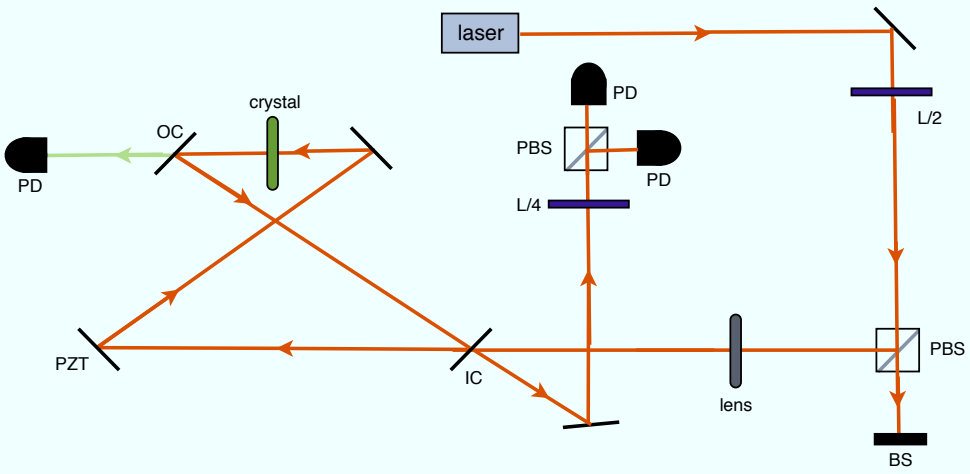

Figure 4.2: Schematic of the green laser system. The slanted black lines are all mirrors. L/2 is a half waveplate, PBS is a polarized beam splitter, BS is a beam stop, L/4 is a quarter waveplate, IC is the input coupler mirror to the cavity, PZT is a flat mirror with a PZT attached to control the length of the cavity, OC is the output coupler mirror, PD are photodiodes. The PD on the far left monitors the transmission signal of the SHG. The other two PDs are connected to the HC lockbox which provides feedback to the PZT.

4.3.2 Optical Elements of the Cavity

A schematic of the optics for the cavity can be seen in Fig. 4.2. Most of the optics in the cavity are mounted on 1″ diameter pillar posts from Thorlabs. The laser beam exits the fiber laser through an adjustable collimating lens and is reflected by a mirror through a half wave plate set to give it vertical polarization. The beam is then split by a polarized beam splitter (PBS). Most of the light is reflected and a portion of it is transmitted through the cube. Currently the transmitted light is sent to a beam stop, however, it can be used to go to the wavemeter or somewhere else desired. The reflected light goes through a lens of focal length 200 mm in order to focus it approximately at the location of one of the waists of the cavity. The beam continues on to partially pass through and partially reflect off of the input coupler (IC) to the cavity. After the beam passes through the IC it follows the bow-tie configuration as shown in Fig. 4.2.

The IC and the other bow-tie mirrors are mounted in 0.5″ Lees mounts which can be bought from LINOS. All of the cavity mirrors were purchased from CVI Melles-Griot. The

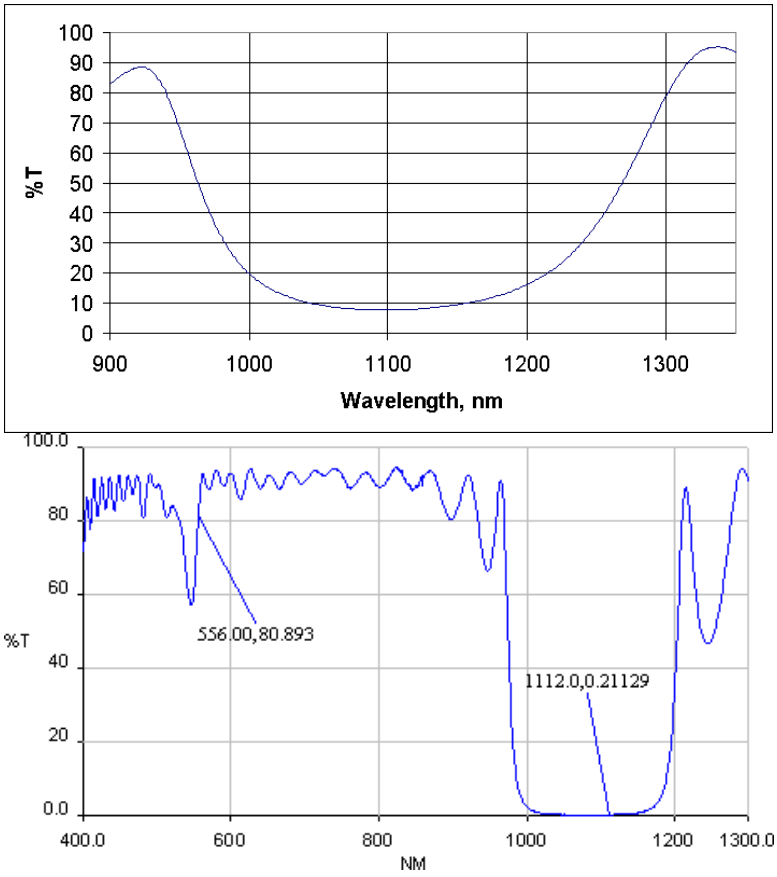

Figure 4.3: Graphs of transmission vs. wavelength of the cavity mirrors as specified by CVI Melles-Griot. The graph on the left is for the input coupler. The right graph is for the other three mirrors which make up the bow-tie configuration.

IC (PR1-1107-92%) has a thickness of 6 mm and is 92% reflective at 1112 nm, see Fig. 4.3. Of the three mirrors other than the IC which make up the bow-tie configuration, two are curved and one is planar. They are made from a BK7 substrate and have been coated to transmit 81% at 556 nm and 0.2% at 1112 nm, see Fig. 4.3. The two curved mirrors (SMCC-0537-0.050-C) have a radius of curvature of 5 cm and are 0.375 in thick. The planar mirror (PW1-0316-C) has a diameter of 8 mm and thickness 4 mm.

The length of the cavity is controlled by a PZT mounted to the planar mirror. This PZT is from Thorlabs (AE0203D04F) it has a change in position of 4.6 ± 1.5 μm at its maximum

drive voltage of 150 V. Currently we are applying a maximum voltage of 90 V which means we can see a maximum of 5 free spectral ranges in the cavity. At the time the PZT was glued to a flat Lees mount the capacitance was 90.2 nF.

Dimensions for the cavity were decided up by using a software called SNLO. This program takes the input of type of crystal, fundamental wavelength, index of refraction, curvature of mirrors, and length of the "legs" of the cavity. The current length of the short leg is approximately 55 mm and the long leg 330 mm. The output of the program tells whether or not the cavity is stable and what the waists of the cavity will be. With the leg dimensions listed above the waist in the crystal is 30.76 μm, which is close to the desired 38 μm calculated at the end of section 3.2.3. The other waist in the cavity is 345.54 μm. SNLO also calculates the index of refraction, d_{eff}, phase matching angle, and walk-off angle for a given crystal. The numbers it gives are consistent with those calculated in section 3.2.2.

The method used for aligning the cavity is as follows. The beam is sent through the IC and centered on the flat mirror attached to the PZT. Then the beam is centered on the first curved mirror and sent through the crystal. The crystal position is adjusted by turning the knobs on its translation stage until the maximum amount of green light is produced. The next step is to center the beam on the second curved mirror, the output coupler (OC). If large adjustments are needed to do this the crystal may have to me moved again. The cavity is closed by trying to overlap the beam from the OC with where the laser passes through the IC. It is necessary to adjust the knobs on the IC and OC to align the reflections on themselves starting with adjusting the IC so the first reflection overlaps the original beam on the PZT mirror. This usually takes many iterations to get a nice looking beam and signal from the detectors.

Currently the light which exits the cavity through the OC goes through a collimating lens and into a detector. Once the cavity is optimized this green light will be split between a spectroscopy and MOT set-up. The cavity's output beam shape and mode is monitored by a CCD camera. This image is created by the IR light which is transmitted by the first curved mirror.

4.4 Locking Scheme and Electronics

The locking scheme for the cavity was developed by Hansch and Couillaud [26]. The light circulating the cavity acquires a frequency dependent phase shift relative to a reference beam taken from the reflection off the IC. The mixture of these two beams is elliptically polarized. They are then sent through a quarter waveplate which separates the beams into two different linear polarizations. They are separated by a PBS and sent into two photodiodes. The photodiodes are glued to a cylinder made from delrin mounted on an aluminum L-shaped stand. The difference of the signals from the two photodiodes creates a dispersion signal.

The subtraction of the photodiode signals and feedback to the PZT is done by the aptly named HC lockbox. This box uses a high voltage power supply to create a sawtooth wave output which is sent to the PZT. Applying this voltage across the PZT effectively sweeps the length of the cavity. While scanning it is possible to see many modes of the cavity and tune the cavity so the desired fundamental TEM_{00} mode is found and maximized. This can be done by looking at the error signal, transmission signal, and/or the image of the beam from the camera. Once a good error signal is seen for the fundamental beam a lock should be obtained. When the cavity is locked the point of zero crossing of the error signal dictates what voltage should be applied across the PZT to hold the length of the cavity fixed.

In order to set the lock flip the switch on the box from sweep to lock. You can get to the desired mode by adjusting the HV offset knob. The Ramp Width knob controls the maximum voltage applied to the PZT. The gain and offset of the photodiodes can also be controlled by the box. The offset determines where the zero crossing of the error signal is. Once a lock is obtained it should be adjusted to get maximum power of the SHG light.

Chapter 5
SPECTROSCOPY AND MOT BEAMS

After the frequency doubled green light exits the cavity it will be taken to the height of the optical table via a periscope. It will then be sent through a half waveplate and a PBS. Of the two beams coming out of the splitter one will be coupled into a fiber and sent to the MOT. The other will go to the spectroscopy set-up.

In order to excite an atomic transition the laser has to be tuned to the precise atomic resonant frequency and remain stable within the linewidth of the transition. To ensure the MOT beams are at the frequencies needed the laser light will be sent through a spectroscopy set-up which will electronically feed back to the laser's PZT. This will allow us to lock the laser to the desired frequency. Here a brief overview of spectroscopy as it applies to our system is given. More extensive descriptions can be found in books such as Foot's *Atomic Physics* [27].

In basic absorption spectroscopy a beam of light, called the probe beam, is sent through a cell filled with an atomic vapor. In our case this is a Hollow Cathode Lamp (HCL) from Hamamatsu (L 2783-70NE-YB). After the beam passes through the cell it is sent to a photodiode. As the frequency of the laser is tuned there will be less light captured at the atomic resonance because some photons will be absorbed by the atoms instead of the detector. This absorption line is Doppler broadened due to the thermal motion of the atoms. As an atom moves in relation to light it sees it blue or red shifted as

$$\omega = \omega_0(1 \pm v/c), \tag{5.1}$$

where in the rest frame of the laser ω is the frequency of the laser, ω_0 is the atomic resonant frequency, and v is the velocity of the atom relative to the light. Equation (5.1) shows the velocity dependence of the frequency of the light.

To reduce Doppler broadening a so-called high intensity pump beam is sent through the cell counterpropagating to the probe beam. This saturates the transition so atoms in

resonance with the pump beam are equally likely to be in the ground and excited state. The density of atoms in the ground state will follow the Maxwell-Boltzmann distribution except for the atoms in the velocity class excited by the pump beam. When the laser is close to resonance both the pump and probe beam interact with the velocity class $v \simeq 0$. Therefore, the the saturation of the absorption by the pump beam reduces the absorption by the probe beam and leads to a narrow peak in the intensity of the probe beam.

If we change the frequency of the pump beam in relation to the probe beam by sending it through an AOM there will still be a velocity class of atoms which interact with both beams. This will be done for future work on the experiment. Modulating the frequency of the pump beam aids in creating an error signal for a lockbox to use in order to provide feedback to the laser's PZT. If the beam is double passed through an AOM it works out that the laser will be locked below the atomic resonant frequency by the frequency of the AOM. Therefore, the frequency of the beam going to the MOT will need to be increased by this amount by sending it through a second AOM.

So far the only step taken towards spectroscopy of the $^1S_0 \rightarrow {}^3P_1$ transition has been looking for absorption of the probe beam. The HCL allows a maximum of 10 mA. When spectroscopy was done with a similar system on the blue $6s^2\ {}^1S_0 \rightarrow 6s6p\ {}^1P_1$ transition it was found that 1.6 mA and 160 V was needed to see absorption. When this was tried with the green $^1S_0 \rightarrow {}^3P_1$ transition no absorption was seen. Absorption vs. current in the HCL for the blue transition was measured and upon comparison of the linewidths of the two transitions ($2\pi \times 29$ MHz blue vs. $2\pi \times 182$ kHz green) it has been concluded more current is needed to see absorption with the green transition. When a search for absorption resumes the current should be increased.

Chapter 6

RESULTS AND FUTURE WORK

6.1 Results

All the pieces of the cavity described in Chapter 4 have been put together to create a bow-tie cavity. We are able to find the fundamental mode and lock to it. However, this lock is not very stable. It lasts for only seconds at a time. Light at 556 nm can be seen when the cavity is locked. Only about 1% of the input beam power comes out of the cavity, this is the same as what was measured for a single pass through the crystal. There is a mixture of IR and green light coming out of this mirror, it is not know what percent is green light.

The enhancement given in (3.48). This can be measured experimentally by measuring the power of the light leaking out of the first curved mirror when the cavity is locked and dividing that by a measurement at the same location when the input coupler is removed. At the time of writing the enhancement is 4. This is very low and must be improved.

The total length of the cavity is 385 mm. This gives a FSR of 780 MHz. The losses in the cavity are mainly due to the IC which leads to a finesse $F = 79$. Dividing these two gives a linewidth $\Gamma = 780$ MHz. Before the laser fiber was damaged measurements of the cavity gave a $F = 66$ and $\Gamma = 11.8$ MHz. Current measurements of the cavity give $F = 16$ and $\Gamma = 50$ MHz. It is unknown if the broad linewidth we are seeing now is because the cavity isn't as well aligned as before or if it is the fault of something else yet to be discovered.

6.2 Future Work

There are several steps to be taken to increase the enhancement of the cavity. Limiting vibrations is essential for a lockable cavity. Although many steps for passive isolation have been made more could be done. A new input coupler would be beneficial. The current mirror was bought at reflectivity of 92% because CVI Melles-Griot had it available at the time. Considering the reflectivity of the other mirrors are and the AR coatings on the

crystal, it is unlikely the cavity is impedance matched. It is also possible that another lens or lens system outside of the cavity will give better mode matching into the cavity.

The current length of the cavity was chosen based on the calculations done by the SNLO program. Although the length of the short and long leg give a stable cavity, they may not be the best choice for our system. Some adjustment of the lengths has been done, but nothing extensive or radically different has been tried.

The beam coming out of the cavity is elongated in the vertical direction. Aside from poor alignment this could be due to astigmatism of the beam created by the curved mirrors. Astigmatism can be partially reduced by making the angle the beam makes with the mirror's optical axis smaller. Currently this angle is about 16°. Angles as small as 8° have been reported [20]. This angle was set larger as a necessity for the beam to make it around the edge of the crystal holder in the bow-tie configuration. Reducing the angle requires changing the cavity dimensions or how the crystal is mounted.

Once a stable, lockable cavity is established work on the spectroscopy set-up may continue. This will lead to a laser which is locked to the 556 nm transition needed to trap Yb in a MOT.

BIBLIOGRAPHY

[1] M. A. Baranov, M. S. Marenko, V. S. Rychkov, and G. V. Shlyapnikov. Superuid pairing in a polarized dipolar Fermi gas. *Phys. Rev. A*, 66:013606, 2002.

[2] K. Gral, L. Santos, and M. Lewenstein. Quantum Phases of Dipolar Bosons in Optical Lattices. *Phys. Rev. Lett.*, 88:170406, 2002.

[3] D. DeMille. Quantum Computation with Trapped Polar Molecules. *Phys. Rev. Lett.*, 88:067901, 2002.

[4] M. Kozlov and L. Labzowsky. Parity vilation effects in diatomics. *J. Phys. B*, 28:1933, 1995.

[5] T. Zelevinsky, S. Kotochigova, and J. Ye. Precision Test of Mass-Ratio Variations with Lattice-Conned Ultracold Molecules. *Phys. Rev. Lett.*, 100:043201, 2008.

[6] D. DeMille, Sainis S., Sage J., Bergeman T., Kotochigova S., and Tiesinga E. Enhanced sensitivity to variation of m_e/m_p in molecular spectra. *Phys. Rev. Lett.*, 100:043202, 2008.

[7] A. N. Nikolov, J. R. Ensher, E. E. Eyler, H. Wang, W. C. Stwalley, and P.L. Gould. Efficient production of ground-state potassium molecules at sub-mK temperatures by two-step photoassociation. *Phys. Rev. Lett.*, 84:246, 2000.

[8] S. Jochim, M. Bartenstein, A. Altmeyer, G. Hendl, S. Riedl, C. Chin, J. Hecker Denschlag, and R. Grimm. Bose-Einstein Condensation of Molecules. *Science*, 302:2101, 2003.

[9] M. Greiner, C. A. Regal, and D. S. Jin. Emergence of a molecular Bose-Einstein condensate from a Fermi Gas. textitNature (London), 426:537, 2003.

[10] M. W. Zwierlein, C. A. Stan, C. H. Schunck, S. M. F. Raupach, S. Gupta, Z. Hadzibabic, and W. Ketterle. Observation of Bose-Einstein Condensation of Molecules. *Phys. Rev. Lett.*, 91:250401, 2003.

[11] A. J. Kerman, J. M. Sage, S. Sainis, T. Bergeman, and D. DeMille. Production of Ultracold, Polar RbCs* Molecules via Photoassociation. *Phys. Rev. Lett.*, 92:033004, 2004.

[12] D. Wang, J. Qi, M. F. Stone, O. Nikolayeva, H. Wang, B. Hattaway, S. D. Gensemer, P. L. Gould, E. E. Eyler, and W. C. Stwalley. Photoassociative Production and Trapping of Ultracold KRb Molecules. *Phys. Rev. Lett.*, 93:243005, 2004.

[13] C. Haimberger, J. Kleinert, M. Bhattacharya, and N. P. Bigelow. Formation and detection of ultracold ground-state polar molecules. *Phys. Rev. A*, 70:021402(R), 2004.

[14] C. C. Bradley, C. A. Sackett, and R. G. Hulet. Bose-einstein condensation of lithium: Observation of limited condensate number. *Phys. Rev. Lett.*, 78:985,1997.

[15] S. R. Granade, M. E. Gehm, K. M. O'Hara, and J. E. Thomas. All-optical production of a degenerate fermi gas. *Phys. Rev. Lett.*, 88:120405, 2002.

[16] Y. Takasu, K. Maki, K. Komori, T. Takano, K. Honday, M. Kumakura, T. Yabuzaki, and Y. Takahashi. Spin-singlet bose-einstein condensation of two-electron atoms. *Phys. Rev. Lett.*, 91:040404, 2002

[17] T. Fukuhara, Y. Takasu, M. Kumakury, and Y. Takahashi. Degenerate fermi gases of ytterbium. *Phys. Rev. Lett.*, 98:030401, 2007.

[18] T. Fukuhara, Y. Takasu, S. Sugawa, and Y. Takahashi. Quantum degenerate fermi gases of ytterbium atoms. *Journal of Low Tamperature Physics*, 148:441, 2007.

[19] R. Maruyama, R. Wynar, M. V. Romalis, A. Andalkar, M. D. Swallows, C. E. Pearson, and E. N. Fortson. Investigation of sub-Doppler cooling in an ytterbium MOT. *Phys. Rev. A*, 68:11403, 2003.

[20] S. Uetake, A. Yamaguchi, S. Kalto, and Y. Takahashi. High power narrow linewidth laser at 556 nm for magneto-optical trapping of ytterbium. *App. Phys. B*, 92:33, 2008.

[21] A. E. Siegman. *Lasers*. University Science Books, 1986.

[22] A.Yariv. *Optical Electronics*. Oxford University Press, 1991.

[23] B. Zysset, I. Biaggio, and P. Gunter. Refractive indicies of orthorhombic $KNbO_3$ I. Dispersion and temperature dependence. *J. Opt. Soc. Am. B*, 9:380, 1992.

[24] I. Biaggio, P. Kerkoc, L. S. Wu, P. Günter, and B. Zysset. Refractive indicies of orthorhombic $KNbO_3$ II. Phase-matching configurations for nonlinear-optical interactions. *J. Opt. Soc. Am. B*, 9:507, 1992.

[25] G. D. Boyd and D. A. Kleinman. Parametric interaction of focused gaussian light beams. *J. Appl. Phys.*, 19:3597 (1968).

[26] T. W. Hansch and B. Couillaud. Laser frequancy stabilization by polarization spectroscopy of a reflecting reference cavity. *Opt. Comm.*, 35:441, 1980.

[27] C. J. Foot. *Atomic Physics*. Oxford University Press, 2006.